

Coupling FHR Core Design with Power Conversion System

Zhiyao Xing
Eugene Shwageraus

University of Cambridge, Department of Engineering, Trumpington Street, Cambridge, CB2 1PZ, United Kingdom
Email: zx227@cam.ac.uk

Abstract - It has been suggested that the prismatic block type Fluoride-salt-cooled High temperature Reactors (FHRs) can benefit from Advanced Gas-cooled Reactors (AGRs) technologies. [1] This paper contributes to the global FHR development effort by investigating an AGR-like FHR concept. Two reference FHR assembly designs is proposed by replacing the CO_2 coolant in a generic AGR with 2LiF-BeF_2 (FLiBe), using UC and UO_2 respectively. A model that couples the core thermal hydraulics design with the balance of plant design has been proposed in this study. Using the model, the optimum core coolant inlet and outlet temperatures, sizes and aspect ratios of the primary and secondary heat exchangers, pumping power required and temperature conditions of the heat transfer loops can be obtained for the proposed FHR designs. It is discovered in this study that the optimum reference core design using UC fuel is able to provide 3246MWe with a coolant pressure loss of 490kPa when operating at the same nominal condition as a generic AGR, increasing the AGR's power level by a factor of 4.9.

I. INTRODUCTION

The Fluoride-salt-cooled High temperature Reactor (FHR) is a graphite moderated, high temperature reactor concept. Two streams of FHR design have been proposed: the pebble bed design and the prismatic block design. The latter has a graphite block core that resembles many design features of the British Advanced Gas-cooled Reactors (AGR). AGRs have been operating safely and reliably for nearly four decades in the UK. They can operate at core outlet temperatures up to 675 °C, highest among reactors in operation worldwide. [2] There is great amount of valuable experience accumulated over decades of AGR operations that can be transferred to benefit FHR development. [1] Also, with the use of molten salt coolant and AGR's online refuelling facilities, a safety case could be envisaged for online refuelling at full-power, which can enhance fuel utilisation. Acknowledging this, a series of studies is being carried out investigating AGR-like FHR designs options. This report is part of that effort.

In the preliminary stage of the FHR design, one of the questions that need to be addressed is: at what power, temperature ranges and pressure conditions should the reactor core and the heat transfer loops be operating. By coupling the core thermal-hydraulic design of FHR core with the design optimisation of the heat exchanger system, this paper presents a simple power conversion system optimisation model to provide answers to this question for the proposed FHR concept using AGR core configuration.

II. REACTOR CORE DESIGN

The Torness AGR core configuration is adopted as the reference FHR core. The core contains 332 fuel channels inside drilled graphite bricks that are locked together with

square graphite keys. Each fuel assembly that sits in a fuel channel contains two concentric graphite sleeves, within which there are eight fuel elements stacked vertically and linked with a central stainless steel tie bar. Each element consists of three circular rings of 36 fuel pins of 14.5mm in diameter. The cladding is stainless-steel tube of 0.38mm thick and 900mm long. [2] UO_2 and UC, are chosen for investigation in this study, other options such as TRISO will also be considered in the future. Figure 1 below shows a 2D model for the reference assembly modelled with Monte-Carlo code Serpent. [3]

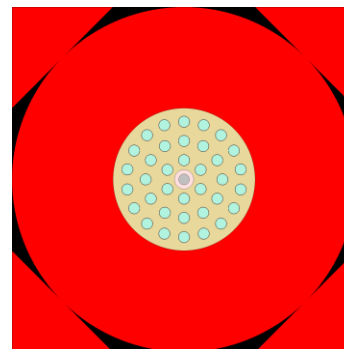


Figure 1. Reference FHR fuel assembly 2D Serpent model. Graphite is shown in red. Coolant flows around the fuel pins and through the central tie bar. The black regions are air gaps which are currently treated as void in the model.

The reference FHR power plant consists of the low-pressure reactor core cooled with 2LiF-BeF_2 (FLiBe), a low pressure intermediate loop filled with NaF-ZrF_4 and a supercritical CO_2 (sCO_2) power cycle. Alternative power conversion cycles and salt candidates for the primary and intermediate loops will be considered in future studies. The intermediate loop creates physical separation between the

nuclear and the power conversion facilities, thus mitigating the potential downstream accident impacts on the reactor core. It also serves as a barrier for Tritium produced in FLiBe; The intermediate molten salt loop can also function as a heat storage during times of low electricity demand. With AGR’s large building structures, the amount of heat that can be stored in the salt can be very large. however, a cost benefit analysis of the addition of the intermediate loop is required, and is aimed to be addressed in future work.

III. CORE THERMAL-HYDRAULIC DESIGN

A calculation sub-routine domainSearch is developed to obtain allowable operating domain the reactor under a specific coolant pressure drop considering temperature safety limits imposed on the reactor components. domainSearch does this by iteratively calling BGCore’s 1D sub-channel thermal-hydraulics module [4] with different reactor power and temperature conditions. Molten salt heat transfer properties used in the BGCore library are taken from INL’s Engineering Database of Liquid Salt Thermophysical and Thermochemical Properties. [5] Reactor axial power profiles are required as inputs for the domainSearch and are obtained by coupled neutronics (Serpent) and thermal-hydraulics (BGCore) calculations.

Temperature safety limits on different components of the core ensure that the reactor operates safely under nominal steady state conditions. Five safety criteria are proposed for the reference FHR designs, as summarized in Table 1. Each safety criterion is derived from a corresponding physical constraint of the reactor. [5] The nominal fuel temperature limit for all proposed FHR designs is derived from that of the Torness AGR: assuming a core radial power peaking factor of 1.3, the maximum fuel temperature of Torness AGR is calculated to be 1420 °C, thus the maximum fuel temperature for the proposed FHRs under nominal operating condition is limited to 1350 °C to allow some margin for the analysis uncertainties.

Table 1. Safety criterion for domain search

Criterion	limit (°C)	Physical Constraints
1. Min bulk $T_{coolant}$	470	Coolant freezing at 459°C
2. Max bulk $T_{coolant}$	700	Hastelloy-N allows 750°C
3. Max local $T_{coolant}$	1000	Coolant boiling at 1430°C
4. Max T_{clad}	1100	SiC failure at 1200°C
5. Max T_{fuel}	1350	AGR max T_{fuel} at 1420°C

Mechanical properties of reactor vessel at high temperature and during transients, and Wigner energy temperature limits of the core graphite impose additional safety requirements. However, these are less limiting requirements than the five considered in Table 1 because of the very large thermal inertia of the core which allows

avoiding rapid temperature changes. Also, high melting temperature of the salt would prevent the accumulation of radiation damage in the graphite.

By implementing these safety limits, domainSearch is able to determine an allowable operating domain and thus the maximum allowable power for the two reference cores for a given assumed pressure drop across the core. Figure 2 illustrates how an operating domain and maximum power allowable are defined using the limiting safety criterion. One such figure and an output file that contains calculations results can be produced with a domainSearch run. The output file can be fed into the power conversion system routine for coupled calculation as explained in later sections.

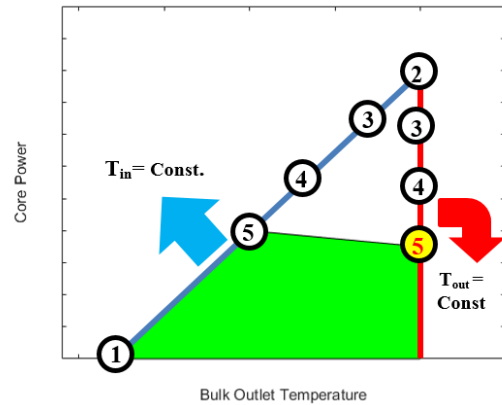


Figure 2. Allowable operation domain using safety limits

The operating domain (green region) is bound by three lines. The blue line that bounds the left side of the domain is the ‘inlet coolant temperature line’; the vertical red line bounding the right side of the domain is the ‘outlet coolant temperature line’; the line bounding the domain from the top is the line joining the most limiting cases from the ‘inlet line’ and the ‘outlet line’. The ‘inlet line’ is determined by fixing the bulk coolant inlet temperature to limiting safety criterion 1, i.e. minimum bulk coolant temperature. Starting from zero power, in which case there is no coolant temperature difference between inlet and outlet, the bulk coolant outlet temperature increases with reactor power. The ‘outlet line’ is determined by fixing the bulk coolant outlet temperature to safety criterion 2, i.e. the maximum bulk coolant temperature. With increasing power, the inlet coolant temperature decreases along the ‘outlet line’. The circled points on the ‘inlet line’ and the ‘outlet line’ represent cases where each of the safety criterion is violated under fixed inlet temperature or fixed outlet temperature conditions, and the numbers in those circles represent the number of the safety criterion violated. Figure 2 illustrates a case where the most limiting safety requirement is the maximum fuel temperature limit. Since a higher outlet temperature would result in a higher thermal efficiency, the maximum power allowable is

determined from the most limiting case on the outlet temperature line, i.e. the yellow circle in Figure 2.

For both UC and UO_2 fuelled cores, consecutive domainSearch runs are performed with core pressure drop (gravitational pressure drop included) reducing from a proposed maximum value of 2 MPa until the the minimum value (gravitational pressure drop only). It is discovered that for the UO_2 fuelled core, with a pressure drop of 1MPa, the maximum allowed core power is 1619 MWt, and the coolant rises $3.14^\circ C$ across the core to $700^\circ C$. With further increase in allowed coolant pressure drop, the improvements in power is not significant for the UO_2 fuelled FHR. This indicates that directly replacing AGR's gas coolant with molten salt does not necessarily result in better performance comparing to Torness AGR (1649 MWt), even at a large coolant pressure drop. This is because for solid fuel FHR designs, the fuel temperature is the most limiting thermal-hydraulic constraint. Replacing gas coolant with salt coolant increases the average coolant temperature, thus reducing the allowable temperature drop between coolant and fuel centre line. This is illustrated in Figure 3, which plots hot channel coolant and maximum fuel temperatures for the reference UO_2 fuelled FHR and AGR with the same power of 1649 MWt. Since the reference UO_2 fuelled FHR uses the same fuel material and configuration as AGR, the temperature rise from coolant to the maximum fuel temperature line is also the same for the two cases. In AGR, CO_2 coolant enters the core at an average temperature of $339^\circ C$, and exits at an average temperature of $639^\circ C$; whereas in the reference FHR, the coolant exits at an average temperature of $700^\circ C$. FLiBe has a much larger ρC_p than CO_2 , thus, the coolant temperature rise in FHR is much smaller than in AGR. As a result, the reference FHR average coolant temperature of the hot channel is around $700^\circ C$, significantly higher than that of the AGR. Therefore, the reference FHR with UO_2 fuel will break the maximum fuel temperature limit with the same operating power as the AGR.

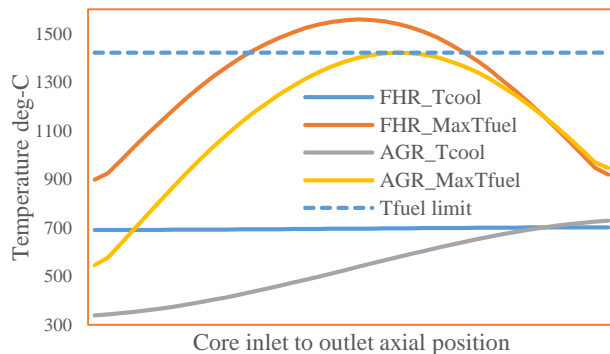


Figure 3. Comparison of hot channel coolant temperatures and maximum fuel temperatures of an AGR at 1649 MWt and the UO_2 fuelled reference FHR design and with 1649 MWt and 300kPa core pressure drop.

For the UC fuelled FHR, with a pressure drop of 2MPa, the core power can reach 8463 MWt power and the coolant temperature rise is $10.64^\circ C$; while with a 168.5 kPa pressure drop, the coolant temperature rise is $100^\circ C$ and the core is allowed a 3624MWt power. The UC fuel more than triples the allowable power rating as compared with the UO_2 case, due to its higher thermal conductivity. For all cases, the maximum allowable power is significantly higher than Torness's 1649MWt. [2] This remarkable increase is a result of superior molten salt heat transfer properties. It is also noted that for all domain searches, the most limiting safety is the maximum fuel temperature, i.e. fuel integrity limit. This indicates that the power output can be further increased by using more advanced fuel forms such as TRISO. From the above analysis, the UO_2 fuelled FHR design is not pursued further in the following analysis of this study.

IV. POWER PLANT LAYOUT

The proposed reference power conversion system consists of the reactor core, primary coolant pumps and heat exchangers, intermediate coolant loop pumps and heat exchangers and a supercritical CO_2 (sCO_2) recompression power cycle. sCO_2 recompression cycle offers one of the highest efficiencies at a given reactor outlet temperatures and has relatively high technology readiness level among all advanced power cycles. After being proposed for advanced reactors use [6], sCO_2 recompression cycle has attracted much attention not only in nuclear but also in other applications such as concentrated solar power, fuel cells, gas turbine exhaust heat recovery systems etc. [7] Studies are also being carried out to improve sCO_2 recompression cycle efficiency and safety [8] Printed Circuit Heat Exchangers (PCHEs) are often proposed to be used in the sCO_2 cycles because the cycle requires relatively large amount of heat to be regenerated and thus, the recuperator becomes one of the major cycle components. PCHE is a commercially available technology and they are currently manufactured by HEATRIC [9].

At the preliminary design stage of the FHR, the 'Advanced Design' recompression sCO_2 power cycle proposed by Dostal et.al is considered because of its high efficiency (45.27%), simplicity, and good compatibility with the proposed FHR temperature conditions. [6] The heat exchangers considered in Dostal et al. sCO_2 recompression cycles are PCHEs. The sizing of the PCHEs in these cycles have been optimised for minimum heat exchanger capital cost. Figure 4 illustrates the power plant layout for the FHR. The thermal power generated from the reactor core is first carried by the reactor coolant to the primary heat exchanger in which the heat is transferred to a secondary coolant. The secondary coolant brings the heat to the power cycle via a secondary heat exchanger. The sCO_2 recompression power cycle includes the secondary exchanger, a turbine, a main compressor, two recuperators, namely, high temperature

recuperator (HTR) and low temperature recuperator (LTR), a heat sink and a compressor. After producing work in the turbine, the hot exhaust CO₂ is directed into both recuperators. The flow of CO₂ is then split into two: one stream goes through the precooler and cold channels of the LTR and recombines with the other stream before going through the HTR. In the Dostal's cycle design, the sCO₂ enters the turbine at a pressure of 19.8MPa and a temperature of 650°C. The main compressor has an inlet pressure of 7.7MPa and an inlet temperature of 32°C.

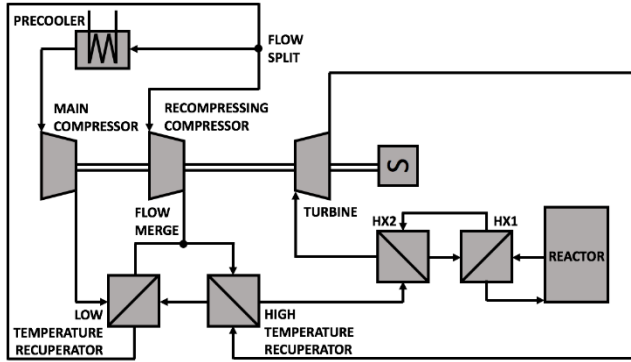


Figure 4. Proposed FHR plant layout

V. HEAT EXCHANGER DESIGN

This section introduces a model for sizing a single heat exchanger for a given operating condition. Heat exchanger capital investment and pump operating cost are the two dominant contributors to the effective total cost of a heat exchanger. A simple heat exchanger sizing model is created in this study to size a PCHE considering economics implications of these two factors. A PCHE simulation subroutine calcHX calculates the required length of a PCHE and its performance given its frontal area, required duty and temperature conditions. A PCHE sizing routine sizeHX then calls calcHX iteratively to find the optimum aspect ratio of the heat exchanger that minimises total cost of the heat exchanger.

1. Heat Exchanger Modelling

PCHEs made with Hastelloy N are proposed as heat exchangers in the reference FHR layout. Hastelloy N shows very good resistance to hot corrosion and can operate at high temperatures of up to 750°C and thus often chosen as material for molten salt environment. PCHEs are made with plates carrying etched channels joined together by diffusion welding to form all-metal modules. A thermal soaking period during the diffusion welding process allows grain growth that gives the PCHE core the strength of its base metal, high pressure containment capability and avoidance of corrosion cells. Also, flow induced vibration problems that happen to traditional shell and tube heat exchangers can also be

avoided. [10] Printed Circuit Heat Exchangers manufactured by HEATRIC have semi-circular etched channels, as shown in Figure 5. The plate thickness and channel width can range from 0.5mm to 5mm. The plates with etched channels can be placed on top of each other with zero or 90° angle to allow concurrent flow, counter current flow or cross flow. Figure 5 presents a cross sectional view of a cross flow PCHE, thus the channels in between the top and bottom channels are invisible in this view. [9] In the Idaho National Laboratory's (INL) feasibility study of secondary heat exchanger concepts for the Advanced High Temperature Reactor (AHTR), [11] a PCHE design was proposed to have a channel width of 3 mm, channel pitch of 3.3mm and a plate thickness of 3.17mm. In the preliminary design stage of the proposed FHR concept, these specifications are adopted in calcHX.

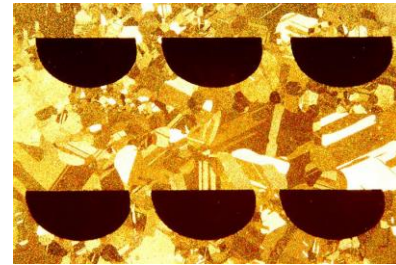


Figure 5. micrograph of a PCHE section. [9]

To model a PCHE of a given duty, Log Mean Temperature Difference (LMTD) and flow area, the lumped parameter heat exchanger routine calcHX uses the LMTD method expressed in equation 1. A counter current flow design is assumed in calcHX in calculating LMTD.

$$Q = U \cdot A \cdot LMTD \quad (1)$$

where Q is the heat exchanger duty, U is the overall heat transfer coefficient and A is the total heat transfer area. Molten salt heat transfer properties are taken from INL's Engineering Database of Liquid Salt Thermophysical and Thermochemical Properties. [5] the Fanning friction factor and the Nusselt number are calculated using Hesselgreaves universal correlations (2001) for PCHE. [10] Several assumptions are made in calcHX: 1) based on Dostal et al. conservative estimations, [6] heat transfer effectiveness of PCHE heat exchangers are assumed to be 98%, and pump efficiency is assumed to be 89%, 2) equal numbers of hot channels and cold channels is assumed, 3) A minimum approach temperature of 25°C is assumed for both heat exchanger units' hot ends, [11] 4) the channels in the PCHE are assumed to have zero waviness, i.e. straight channels, and 5) a single PCHE unit is assumed for each heat transfer stage.

2. Heat Exchanger Sizing

When sizing a heat exchanger, a trade-off exists between the cost of heat exchangers and the cost of pumps. The aspect ratio of the heat exchanger plays an important role in this trade off. For a given duty and LMTD, the smaller the flow area is, the larger the flow velocity and the Reynolds number become, which results in a larger U and a smaller total size of the heat exchanger; however, it also means that a larger pumping power is required. A simplified heat exchanger sizing routine `sizeHX` performs an economic optimisation addressing this trade-off. The heat exchanger upfront capital cost is calculated by multiplying the material cost converted to 2016 currency by a fabrication cost factor of 6.5. [11] A levelized annual heat exchanger capital cost is then calculated assuming a constant annual cash payment over the assumed PCHE service life of 20 years with an interest rate of 5% using the following equation. [13]

$$A = P \left(\frac{i(1+i)^n}{(1+i)^n - 1} \right) \quad (2)$$

where A is the amount of equal annual cash instalments, P is the initial investment, n is the number of service years and i is the discount rate.

The annual cost of pumps is calculated by multiplying the annual pumping power required (assuming a 90% capacity factor of the reactor) by the nuclear power Levelized Cost of Electricity (LCOE) suggested by the Department of Business, Energy & Industrial Strategy [12] converted to 2016 currency. The total levelized annual cost of a heat transfer unit is the sum of the annual heat exchanger cost and the annual pump cost.

The heat exchanger sizing routine `sizeHX` iteratively calls `calcHX` with different total flow areas, and identifies the heat exchanger aspect ratio and size that requires the minimum total levelized annual cost. Figure 6 shows an example of the effect of heat exchanger aspect ratio on the total annual cost of the heat transfer unit. The figure is produced for the primary heat exchanger with an example duty of 6000 MWt and an example LMTD of 36.7°C.

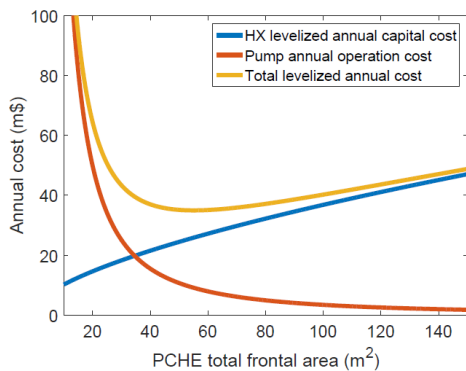


Figure 6. Effect of heat exchanger frontal area on the cost of heat transfer unit.

As can be seen from Figure 6, for a given duty and LMTD, the heat exchanger cost decreases with the increase of total frontal area, while the pumping cost increases with it. The optimum aspect ratio that minimises the annual cost of the heat exchanger can be identified after a complete search of `sizeHX`.

3. Heat Exchanger Simulation and Sizing Code Verification

Before applying the heat exchanger code `calcHX` and sizing routine `sizeHX` to the reference FHR designs to make design recommendations, they must first be verified. Using the same PCHE design specifics, operating conditions and coolant materials as in the INL study [11], `calcHX` successfully reproduced the data published in the INL study report.

E. S. Kim et al [13] described a simplified printed circuit heat exchanger sizing optimisation code based on cost of heat exchanger and pumps, i.e. the same optimisation parameters adapted in this paper. Kim et al performed scaling analysis of printed circuit heat exchanger cost and size and derived a set of analytical equations to determine the optimum heat exchanger size and aspect ratio, hereon referred to as analytical optimisation solutions. These equations are derived based on same fundamental heat transfer and pressure loss equations used in `calcHX` and some simplifying assumptions: 1) the heat exchanger cost calculation assumes no discounting on the capital investment over the service life of heat exchangers and a 100% capacity factor for the reactor. 2) a 100% efficiency of heat transfer was assumed in calculating secondary fluid heat addition and a perfect isentropic efficiency of pumps is also assumed. 3) The code considered frictional pressure loss only when calculating required pumping power. This assumption is also made in the `calcHX` routine. 4) In calculating the overall heat transfer efficiency, the thermal resistance of the heat exchanger wall is assumed to be zero. This is in most cases a valid assumption when the wall thickness is small and the thermal conductivity of the wall material is high so that the wall thermal resistance is normally much smaller than the thermal resistance of the heat transferring fluid. 5) In both `calcHX` and in the analytical optimisation derivations, the longitudinal heat loss was assumed to be zero. The final equations derived in Kim et al's work [13] are summarized below:

$$A_{opt} = \left(\left(\frac{3-b+i}{b} \right) \left(\frac{K_2}{K_1} \right) \right)^{\frac{1}{3+i}} \quad (3)$$

where A_{opt} is the frontal free flow area of the optimised PCHE. The optimum aspect ratio is

$$\frac{H_{opt}}{L_{opt}} = \frac{A_{opt}^{1.5-b}}{\sigma^{1.5} \text{FACT4}} \quad (4)$$

where,

$$K_1 = C_{HXvol}(1-\sigma)\text{FACT4} \quad (5)$$

$$K_2 = C_{pump} Y \left(\frac{\dot{m}_h \text{FACT5}}{\rho_h} + \frac{\dot{m}_c \text{FACT6}}{\rho_c} \right) \quad (6)$$

$$\text{FACT1} = \left(\frac{ak_h}{d_e} \right) \left(\frac{d_e \dot{m}_h}{0.5\mu} \right)^b \text{Pr}_h^c \quad (7)$$

$$\text{FACT2} = \left(\frac{ak_c}{d_e} \right) \left(\frac{d_e \dot{m}_c}{0.5\mu} \right)^b \text{Pr}_c^c \quad (8)$$

$$\text{FACT3} = \frac{1}{(1/\text{FACT1}) + (1/\text{FACT2})} \quad (9)$$

$$\text{FACT4} = \frac{2Q}{\beta \text{FACT3} \text{LMTD}} \quad (10)$$

$$\text{FACT5} = \left[e \left(\frac{d_e \dot{m}_h}{0.5\mu_h} \right)^i \left(\frac{\dot{m}_h^2}{\rho_h} \right) \left(\frac{8}{d_e} \right) \right] \sigma \text{FACT4} \quad (11)$$

$$\text{FACT6} = \left[e \left(\frac{d_e \dot{m}_c}{0.5\mu_c} \right)^i \left(\frac{\dot{m}_c^2}{\rho_c} \right) \left(\frac{8}{d_e} \right) \right] \sigma \text{FACT4} \quad (12)$$

where Q is the heat exchanger duty; σ, β, d_e are the ratio of total frontal flow area to the total frontal area, surface area density and hydraulic diameter of the heat exchanger respectively; ρ, k, μ , and \dot{m} are the density, thermal conductivity, viscosity and mass flow rate of the fluids respectively; the subscript h and c represent hot and cold channel fluids respectively. Parameters a, b, c, e and i are the parameters in the correlations for calculating Nusselt number and friction factor:

$$Nu = aRe^b Pr^c \quad (13)$$

$$f = eRe^i \quad (14)$$

For the selected PCHE base specifications in this study, $\sigma = 0.338$, $\beta = 737.252$ 1/m, $d_e = 1.833$ mm. In the Hesselgreaves universal correlations used in this study, $a = 0.125$, $b = 0.64$, $c = 0.33$, $e = 1.0425$ and $i = -0.76$.

In order to benchmark calcHX with the analytical optimisation solutions, the analytical solutions are modified using the similar assumptions used in calcHX. Assumption 1 and 2 in the analytical optimisation solution are corrected based on the assumptions made in calcHX, i.e. discounting is introduced into the calculation of K_1 based on Equation 2, heat exchanger effectiveness is assumed to be 98% and pump efficiency is assumed to be 89%. Assumption 3 and 5 are also made in calcHX and thus unchanged in the analytical solution derivation. However, assumption 4 is less trivial to be modified as introducing heat exchanger wall thermal resistance into the calculation of overall heat transfer coefficient of the heat exchanger would render the derivation of analytical solutions invalid, and thus was unchanged.

After making these modifications, a PCHE sizing optimisation is performed using both calcHX and the analytical method for an example set up of a primary heat exchanger for the proposed FHR. In this benchmark example, the heat exchanger load is 6000MWt; FLiBe was used as the primary coolant salt which enters the hot channel at 700°C and exits at 640°C. The secondary coolant salt NaF-ZrF4 enters the cold channel at 614°C and exits at 675°C. The size optimisation results using the two methods are presented in Table 2.

Table 2. Benchmarking results for an example primary heat exchanger condition

Parameters	sizeHX	Analytical	error (%)
Min total annual cost(m\$)	47.25	42.74	-10.04
PCHE length (m)	2.37	2.20	-7.68
PCHE volume (m ³)	86.81	75.67	-13.72
Min annual capital cost (m\$)	35.02	30.53	-13.72
Min annual operating cost (m\$)	12.23	12.21	-0.17

As can be seen from the table, the optimum annual costs predicted using sizeHX and the analytical method for the heat exchanger are different by 10.4%. The difference mainly comes from the different optimum annual capital (heat exchanger) cost calculated using the two methods: sizeHX predicts a larger heat exchanger size and thus higher leveled annual cost compared with the analytical method. The differences in the results are speculated to be due to assumption 4 made in analytical optimisation derivation. Assumption 4 overestimates the overall heat transfer coefficient of the heat exchanger and thus, the analytical method would under predict the required heat transfer area and therefore underestimates the required capital investment in heat exchanger. In order to separate and quantify the effects of this assumption and thus validate the optimisation code sizeHX, two more benchmark cases are carried out. 1) molten salt coolants are replaced with CO₂, which has larger thermal resistance and would make assumption 4 more

realistic, and 2) the thermal resistance of the wall is assumed zero in calHX calculation routine.

Table 3 shows the results from the first test. The differences between the results obtained using the two methods are smaller in the CO₂ case. Almost identical (less than 0.1% difference) results are obtained using analytical optimisation solution and calHX. This confirms the suggestion that the difference in optimum PCHE design found by the two methods is the result of assumption 4 used in the analytical solution derivation. Although requiring marginally more computational time than does the analytical method, calHX produces more realistic results for heat exchanger size optimisation.

Table 3. Benchmarking results for an example heat exchanger using CO₂

Parameters	sizeHX	Analytical	error (%)
Min total annual cost(m\$)	68.48	63.93	-6.86
PCHE length (m)	1.32	1.25	-5.27
PCHE volume (m ³)	124.41	113.19	-9.44
Min annual capital cost (m\$)	50.19	45.67	-9.44
Min annual operating cost (m\$)	18.28	18.27	-0.10

VI. COUPLING REACTOR WITH POWER CONVERSION SYSTEM

This section introduces a model to couple the core thermal-hydraulic design with the optimisation of the balance of plant. To illustrate the problem, Figure 7 schematically plots the temperature-entropy (T-S) diagram for the proposed FHR layout. In order to maximise power conversion efficiency, the reactor coolant outlet temperature (point A) is maximised and fixed based on materials safety limit. The temperature and pressure conditions of the turbine inlet of the sCO₂ cycle, point G, (as well as other points in the sCO₂ cycle) are fixed if assuming specific pressure losses along the power cycle. Assuming a minimum approach temperature for all heat exchangers, the intermediate loop salt maximum temperature, point D is also fixed. For a given core coolant pressure drop, relative positions of the reactor inlet (point B) and primary heat exchanger hot channel outlet (point C) on the T-s diagram is fixed. Same analysis applies to the intermediate loop. When plotting the power conversion system T-s diagram to scale, the difference between B and C and the difference between E and F are both too small to distinguish on the diagram. Thus, there are two independent points that need to be optimised in the power conversion system for the proposed FHR. When the reactor coolant temperature increases, i.e. moving B to B' and C to C', less pumping power will be required. However, the reactor thermal power is transferred less efficiently and thus would require more heat transfer surface area in the primary heat

exchanger. Similarly, point E and F on the intermediate loop are also subject to a similar trade-off between secondary heat exchanger size and secondary pumping power. The condition of the reactor loop (point B and C) determines the allowable ranges of LMTDs of the primary and secondary heat exchangers, while the intermediate loop condition (relative position of point E and F with C and H) determines the balance of heat transfer efficiencies of the primary and secondary heat exchanger.

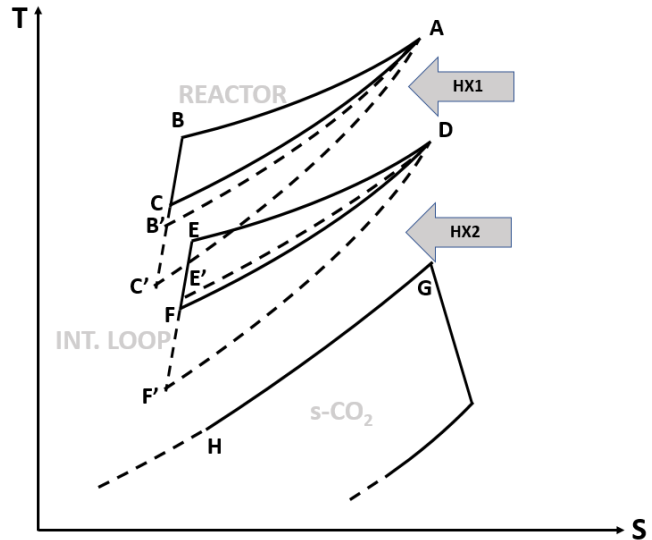


Figure 7. Schematic T-S diagram for the FHR. The relative positions of the points are not to scale.

In order to identify the optimised positions of B, C, E and F, a reactor core and heat exchanger system optimisation code optSys is created. The code flow chart is presented in Figure 8. After determining thermal-hydraulic safety limits, optSys begins by calling the domainSearch sub-routine to determine the maximum allowable power and corresponding coolant temperature conditions for the UC fuelled reference core at an assumed maximum allowable pressure drop of 2MPa. optSys then iteratively calls sizeHX of the primary and secondary heat exchanger to find their optimum designs at different temperature conditions, i.e. systematically moving points B, C, E and F across the allowable range, while optimising heat exchanger designs for the system. optSys performs the heat exchanger system optimisation, while incrementally decreasing core pressure drop until it reduces down to the minimum possible value, i.e. the gravitational pressure drop only. The result from a complete survey of design space for the heat transfer system using optSys stores the optimised heat exchanger system design parameters, such as heat exchanger sizes and aspect ratios, pumping requirements, temperature conditions, etc. for each core pressure drop, or core coolant temperature condition. Figure 9 plots the minimised annual cost of the heat exchanger system and allowable reactor power against core

coolant temperature rise for the UC fuelled FHR by running optSys.

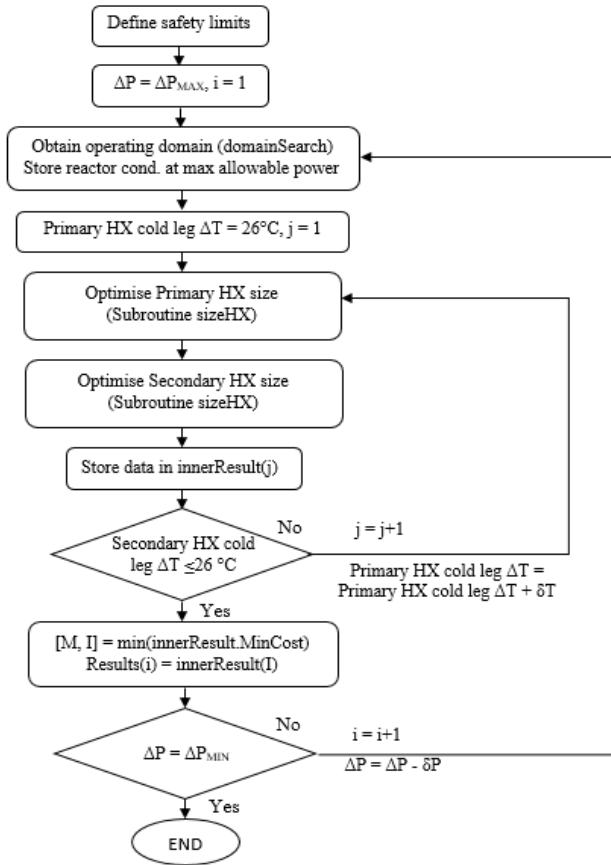


Figure 8. Algorithm for optimising heat exchanger system design

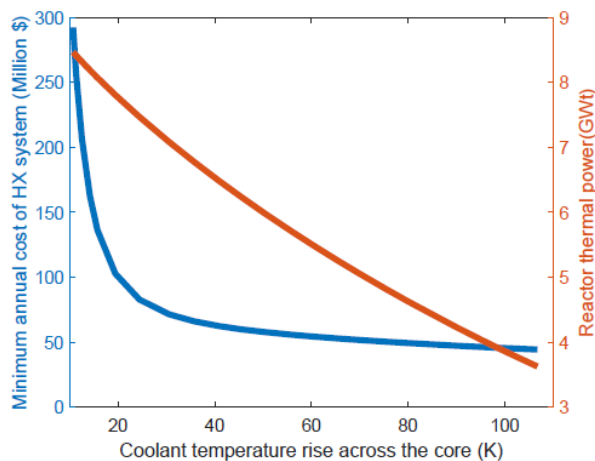


Figure 9. Power conversion system annual cost vs. different core operating conditions

Figure 9 suggests that with smaller reactor coolant temperature rise, i.e. larger pumping power, more power is

allowed. The power almost linearly increases with coolant temperature as the specific heat capacity of FLiBe is not strongly temperature dependent. The total cost of the heat exchanger system increases gradually with coolant temperature increase until a 'threshold' value (~ 20°C) after which the cost increases dramatically. This suggests that the marginal gain in reactor power from the increased pumping power could be cancel by the sharp increase in cost after this threshold. The optimum operating condition should therefore lie at a point around the 'threshold' temperature rise. This sharp increase in cost at the threshold can be explained by Figure 10. When increasing core pressure drop, the achievable core power increases, but the marginal power increase diminishes with the increase of core pressure drop. This is because the improvement in convective heat transfer coefficient with increasing coolant velocity is exploited, and thus core component temperatures becomes increasingly more difficult to be reduced by increasing mass flow rate.

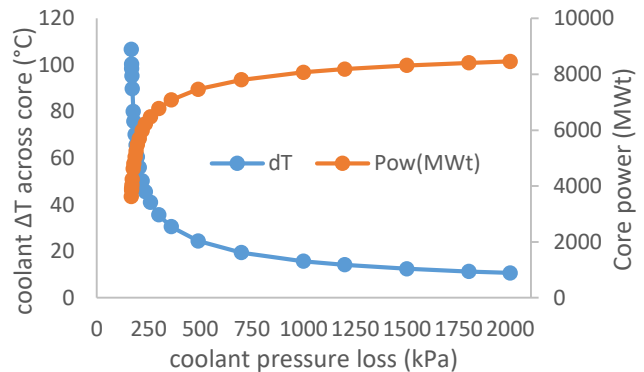


Figure 10. Effect of coolant pressure drop on coolant temperature rise and allowable power

Identification of the actual optimum design for the FHR would require a cost analysis for the whole power conversion system, from the reactor core to the sCO₂ cycle. Assuming that the strike price of the new nuclear power project in Hinckley point C (£92.5/MWh) [14] can be applied to future fleets of nuclear power in the UK, the annual revenue for the plant can be calculated knowing the energy generated by the reactor. The annual cost of electricity can similarly be calculated knowing the LCOE. A slight complication is that the estimated LCOE [12] is applicable to traditional reactors. The FHR proposed in this study is able to generate up to 5.3 times more thermal power and operates at a higher thermal efficiency than the reference Torness AGR without requiring much additional capital investment (which is part of the motivation behind the study). Therefore, when calculating the annual cost of the reference plant, the annual electricity generation from the reference Torness AGR is used assuming 90% capacity factor. To study the effect of heat exchanger system cost on the total annual cost of the plant, all other cost components are assumed to be fixed. The reactor design with the smallest power (3624MWt at 107°C core coolant

temperature increase) is chosen to be the reference design that has the same annual cost as that of the AGR. With this assumption, one is able to calculate the actual annual total cost of the FHR at different operating conditions by adding the difference in the cost of the heat exchanger system to the annual cost of the reference design.

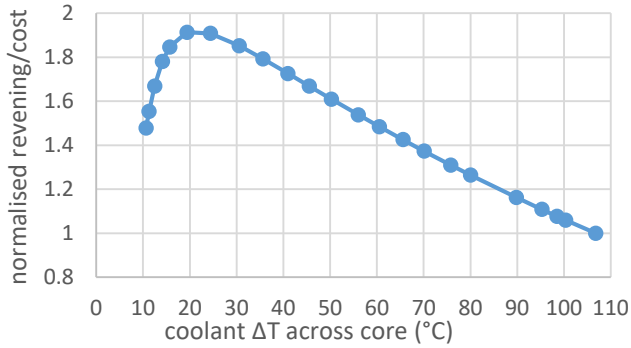


Figure 11. Relative revenue to cost ratio vs core coolant temperature rise

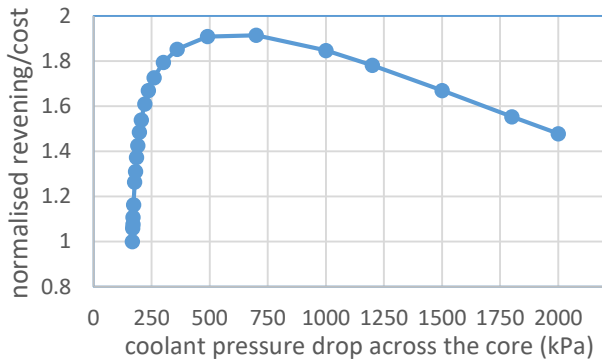


Figure 12. Relative revenue to cost ratio vs coolant pressure drop

Figures 11 and 12 plot the relative annual revenue to cost ratios normalised relative to this reference design. It is shown that at a core temperature rise of around 20°C to 25°C, or equivalently 490kPa to 700kPa core coolant pressure drop, the revenue per cost is maximised. According to the calculation described in this paper, at a 500kPa core pressure drop (25°C coolant temperature increase), the reactor can generate 7467MWt and has a relative annual earning to cost ratio of 1.908; while with 200kPa increase pressure drop, the relative earning to cost ratio improves marginally to 1.914. A large coolant mass flow rate might cause many additional engineering design and material problems. For example, flow induced vibration of the fuel rods is a common phenomenon under large coolant velocity. Therefore, the design with 490kPa is chosen and recommend to the next stage of the FHR study. The detailed specifications of the final recommended design are summarised in Table 4. The

maximum length of a single PCHE module by HEATIC is 1.5m. [13] The recommended heat exchanger designs fit within this the manufacturing limit.

Table 4. Summary of recommended design data for the FHR

Plant Design		
Reactor Type	FHR	
Thermal output	7467	MWt
Electrical output	3246	MWe
Net efficiency	43.48	%
Core Design		
Fuel material	UC	
Moderator material	Graphite	
Coolant material	FLiBe	
Mean core inlet temperature	675	°C
Mean core outlet temperature	700	°C
Core coolant pressure drop	490	kPa
Assembly mass flow rate	382	kg/s
Intermediate Loop Design		
Coolant material	NaF-ZrF ₄	
Mean hot leg temperature	675	°C
Mean cold leg temperature	609	°C
Primary Heat Exchanger Design		
Total volume	75.3	m ³
Total frontal area	73.79	m ³
Heat exchanger length	1.02	m
Log mean temperature difference	42.6	°C
Primary Heat Exchanger Design		
Total volume	62.46	m ³
Total frontal area	44.98	m ³
Heat exchanger length	1.39	m
Log mean temperature difference	60.5	°C

VII. SUMMARY AND DISCUSSION

In this study, a simple computational model containing several verified sub-routines has been developed to couple the core design of an FHR with the design of its power conversion system. The model is able to recommend the optimum core temperature condition that minimises the return on investment of the proposed FHR power plant.

To simplify the problem, the heat exchanger simulation sub-routine calcHX developed in this study considered only frictional pressure loss of fluid in heat exchangers with a fouling factor of 1 when calculating required pumping power, where in fact there are, although relatively small in value,

pressure losses of other types in other components of the power system. This will result in a small under-prediction of operating cost of the reactor. Also, correlations implemented in the code will be subject to future sensitivity study. In addition, plant specific power conversion system complications such as piping length have not been included in this analysis. These simplifications would make the optimisation results to slightly deviate from the real optimum point. In this study, the sCO₂ recompression cycle is assumed to have the same performance for all reactor power outputs. However, this will not be true as larger power implies larger heat exchangers are needed and thus the sCO₂ would lose more energy to the increased friction in the heat exchangers. Thus, the heat exchanger sizing sub-routine will be incorporated into the simulation of sCO₂ power cycle in future studies to provide more realistic estimations of the optimum reactor core and balance of plant design.

This study is an incremental step in a series of investigations into AGR-like FHR designs options: to assist in performing core and power system thermal-hydraulics design and to narrow down design options for future neutronics designs. Despite some simplifications made in the analysis of this complicated problem, the model presented in this paper provides valuable insights and useful results for preliminary design of proposed FHR concepts. The model was applied to the reference UC fuelled FHR core design with a sCO₂ power cycle and the result of the model will be used as inputs for the future core neutronics analysis in the continual study of FHR. The model can be easily expanded for application to other reactor designs and power cycles. With little modification, the model can also be used to perform cost benefit analysis of the intermediate loop. If the Tritium problem proves to be difficult for FHRs, the results of such an analysis could be of significant value.

REFERENCES

1. C. FORSBERG, J. RICHARD, J. POUNDERS, R. KOCHENDARFER, K. STEIN, E. SHWAGERAUS, and G. PARKS, "Development of a Fluoride-Salt-Cooled High-Temperature Reactor (FHR) Using Advanced Gas-Cooled Reactor Technology," *ANS Summer Meeting*, (2015).
2. E. NONBEL, "Description of the Advanced Gas Cooled Type of Reactor," Rise National laboratory, Roskilde, Denmark, (1996).
3. J. LEPPÄNEN, "Serpent – a Continuous-energy Monte Carlo Reactor Physics Burnup Calculation Code," VTT Technical Research Centre of Finland, (2015).
4. Y. SHAPOSHNIK et al, "Thermal-Hydraulic Feedback module for BGCore system," *Proc. 25th Conferences of the Nuclear Societies in Israel*, Dead Sea, Israel.
5. M. S. SOHAL, M. A. EBNER, P. SABHARWALL, and P. SHARPE "Engineering Database of Liquid Salt Thermophysical and Thermalchemical Properties," Idaho National laboratory, Idaho Falls, United States, (2010).
5. R. R. ROMATOSKI, W. HU, and C. W. FORSBERG "Thermal Hydraulic Licensing Limits for a Prismatic Core Fluoride Salt Cooled High Temperature Reactor," Pergamon Press, (2001).
6. V. Dostal, M.J. Driscoll, P. Hejzlar, "A Supercritical Carbon Dioxide Cycle for Next Generation Nuclear Reactors," Massachusetts Institute of Technology, Cambridge (MA), (2004)
7. Y. AHN, S. J. BAE, M. KIM, S. K. CHO, S. BAIK, J. I. LEE, and J. CHA, "Review of Supercritical CO₂ Power Cycle Technology and Current Status of Research and Development," *Nuclear Engineering and Technology*, 47 647-661 (2015).
8. W. S. JEONG, J. I. LEE, Y. H. JEONG, "Potential Improvements of Supercritical Recompression CO₂ Brayton Cycle by Mixing Other Gases for Power Conversion System of a SFR," *Nuclear Engineering and Design*, 241 2128-2137 (2008).
9. D. SOUTHALL, R. L. PIERRES, and S. J. DEWSON, "Design Considerations for Compact Heat Exchangers," *Proc. ICAPP 2008*, Anaheim, CA, June 8–12, 2008, Paper 8009 (2008)
10. J. E. HESSELGREAVE, "Compact Heat Exchangers: Selection, Design and Operation," p. 25, A. KRAMDEN, Ed., American Nuclear Society, La Grange Park, Illinois (2008).
11. P. SABHARWALL, E. S. KIM, A. SIAHPUSH, N. ANDERSON, M. GLAZOFF, B. PHOENIX, R. MIZIA, D. CLARK, M. MCKELLAR, and M. W. PATTERSON, "Feasibility Study of Secondary Heat Exchanger Concepts for The Advanced High Temperature Reactor," Idaho National laboratory, Idaho Falls, United States, (2011).
12. DEPARTMENT FOR BUSINESS, ENERGY & INDUSTRIAL STRATEGY "Electricity Generation Costs," HM Government (2015).
13. E. S. KIM, C. H. OH, S. SHERMAN "Simplified Optimum sizing and Cost Analysis for Compact Heat Exchanger in VHTR," *Nuclear Engineering and Design*, 238 2635 – 2647 (2008).
14. SECRETARY OF STATES FOR BUSINESS, ENERGY & INDUSTRIAL STRATEGY "Hinkley Point C Value for Money," HM Government (2015).